HMGB1 released from nociceptors mediates inflammation

Huan Yang[a,1,2], Qiong Zeng[a,1], Harold A. Silverman[a], Manojkumar Gunasekaran[a], Sam J. George[a], Alex Devarajan[a], Meghan E. Addorisio[a], Jianhua Li[a], Téa Tsaava[a], Vivek Shah[a], Timothy R. Billiar[b], Haichao Wang[c], Michael Brines[a], Ulf Andersson[d], Valentin A. Pavlov[a,e,f], Eric H. Chang[a,e,f], Sangeeta S. Chavan[a,e,f,2], and Kevin J. Tracey[a,e,f,2]

[a]Laboratory of Biomedical Sciences, Institute of Bioelectronic Medicine, Feinstein Institutes for Medical Research, Northwell Health, Manhasset, NY 11030; [b]Department of Surgery, University of Pittsburgh Medical Center, Pittsburgh, PA 15213; [c]Institute of Molecular Medicine, Feinstein Institutes for Medical Research, Northwell Health, Manhasset, NY 11030; [d]Department of Women's and Children's Health, Karolinska Institute, Karolinska University Hospital, 17176 Stockholm, Sweden; [e]The Elmezzi Graduate School of Molecular Medicine, Manhasset, NY 11030; and [f]Donald and Barbara Zucker School of Medicine at Hofstra University, Hempstead, NY 11549

Edited by Lawrence Steinman, Stanford University School of Medicine, Stanford, CA, and approved June 17, 2021 (received for review February 1, 2021)

Inflammation, the body's primary defensive response system to injury and infection, is triggered by molecular signatures of microbes and tissue injury. These molecules also stimulate specialized sensory neurons, termed nociceptors. Activation of nociceptors mediates inflammation through antidromic release of neuropeptides into infected or injured tissue, producing neurogenic inflammation. Because HMGB1 is an important inflammatory mediator that is synthesized by neurons, we reasoned nociceptor release of HMGB1 might be a component of the neuroinflammatory response. In support of this possibility, we show here that transgenic nociceptors expressing channelrhodopsin-2 (ChR2) directly release HMGB1 in response to light stimulation. Additionally, HMGB1 expression in neurons was silenced by crossing synapsin-Cre (Syn-Cre) mice with floxed HMGB1 mice (HMGB1$^{f/f}$). When these mice undergo sciatic nerve injury to activate neurogenic inflammation, they are protected from the development of cutaneous inflammation and allodynia as compared to wild-type controls. Syn-Cre/HMGB1$^{fl/fl}$ mice subjected to experimental collagen antibody–induced arthritis, a disease model in which nociceptor-dependent inflammation plays a significant pathological role, are protected from the development of allodynia and joint inflammation. Thus, nociceptor HMGB1 is required to mediate pain and inflammation during sciatic nerve injury and collagen antibody–induced arthritis.

HMGB1 | cytokine | arthritis | DAMP | sciatic nerve injury

The dual threat of infection and injury exerted a significant influence on the evolution of the mammalian immune and nervous systems. The nervous system detects changes in the environment, generates reflexive responses to those changes, and integrates these responses across space and time to establish adaptive memories of events (1, 2). Sensory neurons, termed nociceptors, innervate tissues subjected to infection and injury and are activated by the molecular products of microbes and tissue injury (3–6). Nociceptor signaling stimulates reflexive neural circuits to coordinate defensive behavior, including inflammation (3–9). Reflex neural signaling arising in the brain and spinal cord is capable of integrating divergent stimulating and inhibitory inputs, because neural signaling circuits act in opposition (10, 11). This balance of opposing signals enables fine tuning of physiological responses by smoothing gradients of corrective action in response to a changing environment (12). Evolutionary pressure from infection and injury also molded the mammalian immune system to detect changes in the environment, mobilize coordinated defensive reactions, and establish memory (13). The acute onset of infection and injury produces inflammation, defined by pain, edema, heat, redness, and loss of function mediated by immune cells producing cytokines and other inflammatory mediators (6, 14). Because uninhibited inflammation also causes dangerous shock and lethal tissue injury, homeostatic mechanisms at the intersection of the nervous system and immune system have a fundamental role in health by inhibiting inflammation (15–17).

The nervous system inhibits inflammation by transmitting antiinflammatory signals in the vagus nerve, which arises in the brainstem and sends efferent projections to the organs (15–18). In the inflammatory reflex, signals descend from the brain to the abdominal celiac mesenteric ganglia, the origin of the splenic nerve (19, 20). In the spleen, splenic nerve signals stimulate a subset of T lymphocytes to secrete acetylcholine, which interacts with alpha 7 nicotinic acetylcholine receptors to inhibit macrophage production of TNF and other inflammatory mediators (21–23). Detailed mechanistic insight into the neuroscience, functional immunology, and molecular mechanisms of the inflammatory reflex enabled therapeutic trials using vagus nerve stimulation to inhibit inflammation in humans. This strategy to stimulate the inflammatory reflex inhibits cytokine release and suppresses inflammation in patients with inflammatory bowel disease and rheumatoid arthritis (24–26).

Significance

Nociceptors are sensory neurons that detect changes in the body's internal and external milieu. Although occupying a primary role in signaling these changes to the nervous system, nociceptors also initiate neurogenic inflammation by sending antidromic signals back into the tissue. Because HMGB1 is a well-characterized endogenous mediator, which stimulates inflammation and is expressed by neurons, we reasoned HMGB1 release may be an important component of neurogenic inflammation. Here, by combining optogenetics, neuronal-specific ablation, nerve-injury, and inflammatory disease models, with direct assessment of inflammation and neuropathic pain, we show that nociceptor HMGB1 is required for an inflammatory response. These results provide direct evidence that nociceptor-related pain and inflammation can be prevented by targeting HMGB1.

Author contributions: H.Y., U.A., S.S.C., and K.J.T. designed research; H.Y., Q.Z., M.G., S.J.G., A.D., M.E.A., T.T., and V.S. performed research; J.L. and T.R.B. contributed new reagents/analytic tools; H.Y. and U.A. analyzed data; and H.Y., H.A.S., H.W., M.B., U.A., V.A.P., E.H.C., S.S.C., and K.J.T. wrote the paper.

The authors declare no competing interest.

This article is a PNAS Direct Submission.

[1]H.Y. and Q.Z. contributed equally to this work.

[2]To whom correspondence may be addressed. Email: HYang@northwell.edu, schavan@northwell.edu, or kjtracey@northwell.edu.

This article contains supporting information online at https://www.pnas.org/lookup/suppl/doi:10.1073/pnas.2102034118/-/DCSupplemental.

Published August 12, 2021.

Since evolution selects for reflexively controlled homeostatic systems acting antagonistically, here we reasoned it likely also selected for neural reflex circuits which stimulate inflammation and enhance immunity.

High mobility group box 1 protein (HMGB1), a ubiquitous nuclear protein conserved across evolution from archaea to mammals, is a necessary and sufficient mediator of sterile injury- and infection-elicited inflammation and immunity (27, 28). It is passively released by cells undergoing necrosis and secreted by innate immune cells activated by inflammation (27, 29). HMGB1 stimulates inflammation by activating the receptor for advanced glycation end products (RAGE) and Toll-like receptor 2, 4, and 9 (TLR 2, 4, and 9) expressed by many different cell types (30–32). Signal transduction via these receptors culminates in increased expression of cytokines, and in recruiting and stimulating monocytes, lymphocytes, and neutrophils. HMGB1 also stimulates dendritic cell maturation and enhances antibody responses to antigen, an important early stage in memory formation (33, 34). Administration of HMGB1 antagonists significantly attenuates the severity of inflammation in preclinical models of sepsis, inflammatory bowel disease, arthritis, and neuroinflammation (31, 32, 35, 36).

HMGB1 is expressed in the nervous system in cortical neurons and in nociceptors (37–40). In preclinical models of nerve injury, HMGB1 levels are increased in the cell bodies of nociceptors residing in the dorsal root ganglia (DRG) (39, 40). In brain neurons, HMGB1 translocates into the cytoplasm and is released during ischemia (38, 41). Exposure of cortical neurons to ethanol activates HMGB1 release via a mechanism dependent upon NOX2/NLRP1 inflammasome (42). Neuronal HMGB1 expression is also significantly enhanced during nerve injury (39, 43, 44). Because HMGB1 stimulates inflammation, and is expressed by nociceptors, and since nociceptors provide a ubiquitous network of nervous system connectivity to peripheral tissues, we reasoned HMGB1 released by nociceptors is a mechanism of neurogenic inflammation. Here, utilizing neuronal-specific ablation of HMGB1 (Syn-Cre/HMGB1$^{fl/fl}$ mice), we discovered a specific role for neuron-derived HMGB1 in inflammation. Genetic silencing of HMGB1 in neurons attenuates inflammation after sciatic nerve injury and in collagen antibody–induced polyarthritis revealing a previously unexpected, but essential, mechanistic role for neuronal HMGB1 in inflammation.

Results and Discussion

HMGB1 Is Actively Released by Stimulated Sensory Neurons. HMGB1 expression is up-regulated during nerve and tissue injury, but the cellular source and function of HMGB1 was previously unknown. We used an optogenetic approach to investigate whether stimulated neurons release HMGB1 upon activation. Channelrhodopsin-2 (ChR2) is a light-gated ion channel that is activated by exposure to blue light (45). To selectively activate sensory neurons, we generated transgenic Vglut2-Cre/ChR2-eYFP mice that express ChR2 coupled to an enhanced yellow fluorescent protein (ChR2-eYFP) directed by vesicular glutamate transporter type 2 (VGlut2) promoter. VGlut2 is expressed in peripheral glutamatergic sensory neurons (46). Sensory neurons harvested from the DRG of Vglut2-Cre/ChR2-eYFP mice were cultured and stimulated with 470 nm light in vitro. Consistent with previous reports (40), quiescent sensory neurons constitutively express HMGB1 and maintain an intracellular pool of HMGB1 predominantly in the nucleus (Fig. 1*A*, optogenetic control). Sixty minutes after acute optogenetic activation, significant levels of HMGB1 are observed in the cytoplasm of sensory neurons (Fig. 1*A*, optogenetic stimulated), confirming that stimulated nociceptors translocate nuclear HMGB1 to the cytoplasm before releasing it into the extracellular milieu. We observe a time-dependent increase in the extracellular HMGB1 levels after optogenetic stimulation of nociceptors (Fig. 1*B*). In contrast, photostimulation of DRG sensory neurons from Vglut2-Cre/ChR2-eYFP mice using yellow light (595 nm), which does not activate ChR2, fails to induce HMGB1 release (Fig. 1*B*, control). Lactate dehydrogenase (LDH), a soluble cytoplasmic enzyme released upon membrane disruption or cell death (47), is not released during light exposure (Fig. 1*C*), further confirming that HMGB1 is actively secreted by stimulated nociceptors.

Generation and Characterization of Syn-Cre/HMGB1$^{fl/fl}$ Mice. To investigate the functional role of nociceptors and HMGB1 in inflammation, we selectively ablated HMGB1 expression in neurons by crossing synapsin-Cre (Syn-Cre) mice with floxed *Hmgb1* mice (HMGB1$^{f/f}$) (*SI Appendix*, Fig. S1*A*). Although global deletion of *Hmgb1* leads to early postnatal death (48), mice lacking HMGB1 expression in neurons (Syn-Cre/HMGB1$^{fl/fl}$) develop normally. No significant differences are observed in body weights of 8- to 10-wk-old Syn-Cre/HMGB1$^{fl/fl}$ mice as compared to age- and sex-matched wild-type (WT) and HMGB1$^{fl/fl}$ control mice (*SI Appendix*, Fig. S1*B*). Specific genetic ablation of HMGB1 expression in neurons significantly depletes HMGB1 protein levels in DRG sensory neurons in Syn-Cre/HMGB1$^{fl/fl}$ mice as compared to WT and HMGB1$^{fl/fl}$ mice (*SI Appendix*, Fig. S1 *C* and *D*). Immunostaining of the cultured DRG neurons confirms absence of HMGB1 in the nucleus of Syn-Cre/HMGB1$^{fl/fl}$ sensory neurons as compared to WT (*SI Appendix*, Fig. S1*E*). In addition, HMGB1 expression is nondetectable in the brain, but abundant in splenic immune cells in Syn-Cre/HMGB1$^{fl/fl}$ mice (*SI Appendix*, Fig. S1 *F* and *G*).

Neuronal HMGB1 Ablation Leads to Reduced Local Inflammation and Hyperalgesia after Sciatic Nerve Injury. To test whether neuronal HMGB1 is required for mediating tissue inflammation following nerve injury, we utilized ligature constriction of the sciatic nerve, a standard preclinical model, which produces inflammation, swelling, and hyperalgesia in the paw (49, 50). Syn-Cre/HMGB1$^{fl/fl}$ and control WT and HMGB1$^{fl/fl}$ mice were subjected to sciatic nerve injury (49). HMGB1 is significantly increased in paw tissue from WT and HMGB1$^{fl/fl}$ control mice (Fig. 2 *A* and *B*), while Syn-Cre/HMGB1$^{fl/fl}$ mice do not exhibit increased paw HMGB1 expression (Fig. 2 *A* and *B*). Following sciatic nerve injury, proinflammatory cytokine levels in paw tissues are significantly elevated in WT and HMGB1$^{fl/fl}$ control mice, whereas a significant reduction is observed in Syn-Cre/HMGB1$^{fl/fl}$ as compared to HMGB1$^{fl/fl}$ mice (HMGB1$^{fl/fl}$ mice; CXCL1: 206 ± 10, TNF: 241.7 ± 44, IL-18: 340 ± 91 vs. Syn-Cre/HMGB1$^{fl/fl}$ mice; CXCL1: 66 ± 6 [$P < 0.0001$], TNF: 84.3 ± 10.9 [$P < 0.05$], IL-18: 136.3 ± 22 pg/mg protein) (Fig. 2 *C*–*E*). No significant differences in CXCL1, TNF, and IL-18 levels are observed between WT and HMGB1$^{fl/fl}$ mice following sciatic nerve injury (Fig. 2 *C*–*E*). Next, we examined mechanical hypersensitivity (allodynia) in Syn-Cre/HMGB1$^{fl/fl}$ mice to analyze the contribution of neuronal HMGB1 in developing mechanical hyperalgesia, a cardinal feature of inflammation. Mechanical hyperalgesia after sciatic nerve injury is significantly reduced in Syn-Cre/HMGB1$^{fl/fl}$ mice as compared to WT and HMGB1$^{fl/fl}$ control mice (threshold responses in sciatic nerve injury groups: WT = 0.48 ± 0.03, HMGB1$^{fl/fl}$ = 0.53 ± 0.1, Syn-Cre/HMGB1$^{fl/fl}$ = 1.11 ± 0.06 g, $P < 0.0001$ vs. HMGB1 $^{fl/fl}$) (Fig. 2*F*).

These data indicate neuronal HMGB1 is required to mediate nerve injury–induced tissue inflammation and neuropathic pain. Following sciatic nerve injury, a partial denervation of the skin occurs (51), followed by variable regeneration and sprouting from adjacent nociceptors and recruitment of inflammatory cells, which may be another cellular source of HMGB1.

Anti-HMGB1 mAb Administration Ameliorates Sciatic Nerve Injury–Induced Hyperalgesia. Since neuronal HMGB1 is strongly correlated with inflammation and hyperalgesia following nerve injury, we tested whether neutralizing HMGB1 ameliorates sciatic nerve injury–induced hyperalgesia. Administration of monoclonal

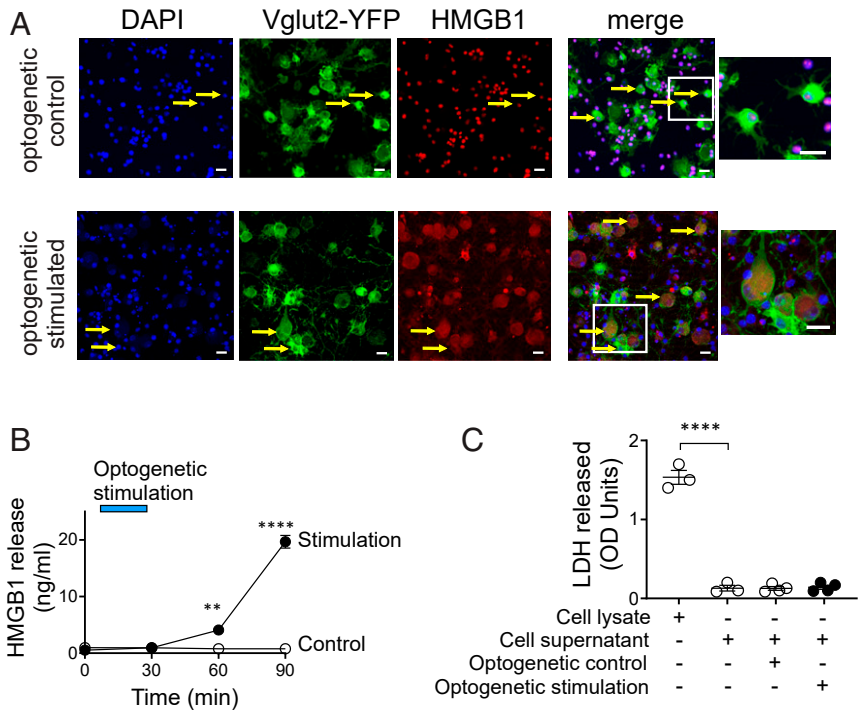

Fig. 1. HMGB1 is actively released by stimulated sensory neurons. (*A* and *B*) Optogenetic stimulation of sensory neurons induces HMGB1 release. DRG neurons harvested from VGlut2-ChR2-YFP mice were stimulated with control yellow light (595 nm, $n = 3$) or blue light (470 nm, $n = 4$) at 20 Hz, 10% duty cycle for 30 min. (*A*) Confocal images showing translocation of HMGB1 from the nucleus to the cytoplasm. Fixed sensory neurons are stained with DAPI (blue), YFP (green, expressed in glutamatergic neurons), and anti-HMGB1 (red). The *Inset* shows the merged images of DAPI, YFP, and HMGB1 staining. Note the strong cytoplasmic translocation of HMGB1 in the sensory neurons stimulated with blue light, whereas neurons stimulated with control light exhibit predominant nuclear expression. (Scale bars, 20 μm.) Data are representative of three independent experiments. (*B*) Sensory neurons release HMGB1 upon activation. Blue bar indicates the duration of optogenetic stimulation. A time-dependent increase in secreted HMGB1 levels is observed following optogenetic stimulation of sensory neurons. Data are represented as mean ± SEM. Two-way ANOVA followed by Sidak's multiple comparisons test between groups: control vs. blue light stimulation (at 60 min: $^{**}P < 0.01$, at 90 min: $^{****}P < 0.0001$). (*C*) Optogenetic stimulation does not induce neuronal cell death. Cell viability was measured by LDH release. Cell lysate was included as a positive control for LDH measurements. $n = 3$ to 4 separate experiments, and each performed in duplicate. Data are represented as individual experimental data point with mean ± SEM. One-way ANOVA followed by Tukey's multiple comparisons test between groups: $^{****}P < 0.0001$.

anti-HMGB1 antibody (anti-HMGB1 mAb) (52) to rats (300 μg/rat, intraperitoneally [i.p.]) attenuates sciatic nerve injury–induced mechanical hypersensitivity (Fig. 3*A*). Significant improvement occurs in a dose-dependent manner in animals receiving anti-HMGB1 mAb (anti-HMGB1 mAb [300 μg/rat] = 2.3 ± 0.2 vs. IgG [300 μg/rat] = 0.9 ± 0.1 g, $P < 0.0001$) (Fig. 3*A*). Sciatic nerve injury also produces thermal hypersensitivity, a sign of inflammation-induced hyperalgesia (53). Significant increases in the paw withdrawal latency are observed in the treated animals in an antibody dose-dependent manner as compared to controls (IgG vs. anti-HMGB1 mAb [300 μg/rat]: 4.1 ± 0.2 vs. 7.2 ± 0.3 s, $P < 0.0001$) (Fig. 3*B*). To determine whether increased amounts of mAb could improve over the 300 μg/rat dose initially tested, additional MAb doses were administered on successive days to rats (Fig. 3 *C* and *D*) and mice (*SI Appendix*, Fig. S2 *A* and *B*). The results show that additional doses provide no further improvement over the initial single dose. Additionally, a significant reduction is observed in thermal hypersensitivity in rats receiving anti-HMGB1 mAb (Fig. 3*E*). These results indicate antibody neutralization of extracellular HMGB1 following nerve injury attenuates inflammatory hyperalgesia.

Ablation of Neuronal HMGB1 Reduces Joint Inflammation and Cartilage Destruction and Improves Hyperalgesia in Murine Collagen Antibody–Induced Arthritis. HMGB1 levels are significantly increased in synovial tissues and synovial fluid in experimental models of arthritis and in patients with rheumatoid arthritis and tendonitis (54–56). HMGB1-specific antagonists attenuate joint inflammation in several preclinical models of arthritis (54, 57). To investigate the role of neuronal HMGB1 in the pathogenesis of arthritis, we utilized a clinically relevant collagen antibody–induced arthritis (CAIA) mouse model (58). In this model, both pain and the development of arthritis depend upon nociceptor-induced neuroinflammation (59, 60). Following anti-collagen antibody administration, both male and female WT and HMGB1$^{fl/fl}$ control mice develop polyarthritis, as indicated by increased swelling of ankle joints and paws (Fig. 4*A*), elevated arthritis scores (Fig. 4*B*, *SI Appendix*, Fig. S3*A*), and mechanical hypersensitivity (Fig. 4*C*, *SI Appendix*, Fig. S3*B*). No significant difference in the severity of arthritis score is observed between WT and HMGB1$^{fl/fl}$ mice (Fig. 4*B*). However, a significantly delayed onset and reduced severity of polyarthritis occurs in Syn-Cre/HMGB1$^{fl/fl}$ mice of both genders (Fig. 4 *A* and *B*, *SI Appendix*, Fig. S3*A*). This is accompanied by a significant reduction in mechanical hyperalgesia (Fig. 4*C*, *SI Appendix*, Fig. S3*B*).

Proinflammatory cytokine and chemokine levels are significantly increased in the inflamed paw tissues in both male and female WT and HMGB1$^{fl/fl}$ mice (Fig. 4 *D–I*, *SI Appendix*, Fig. S3 *D–H*). HMGB1 levels are also significantly increased in the inflamed paw tissues in both male and female WT and HMGB1$^{fl/fl}$ mice, but not in Syn-Cre/HMGB1$^{fl/fl}$ mice (male mice: WT = 1.9 ± 0.2, HMGB1$^{fl/fl}$ = 2.1 ± 0.3 vs. Syn-Cre/HMGB1$^{fl/fl}$ = 0.8 ± 0.1 ($P < 0.0001$) (Fig. 4*D*, *SI Appendix*, Fig. S3 *C* and *D*). Chemokine and cytokine levels in the arthritic paw tissues are significantly elevated in WT and HMGB1$^{fl/fl}$ control mice, whereas these levels

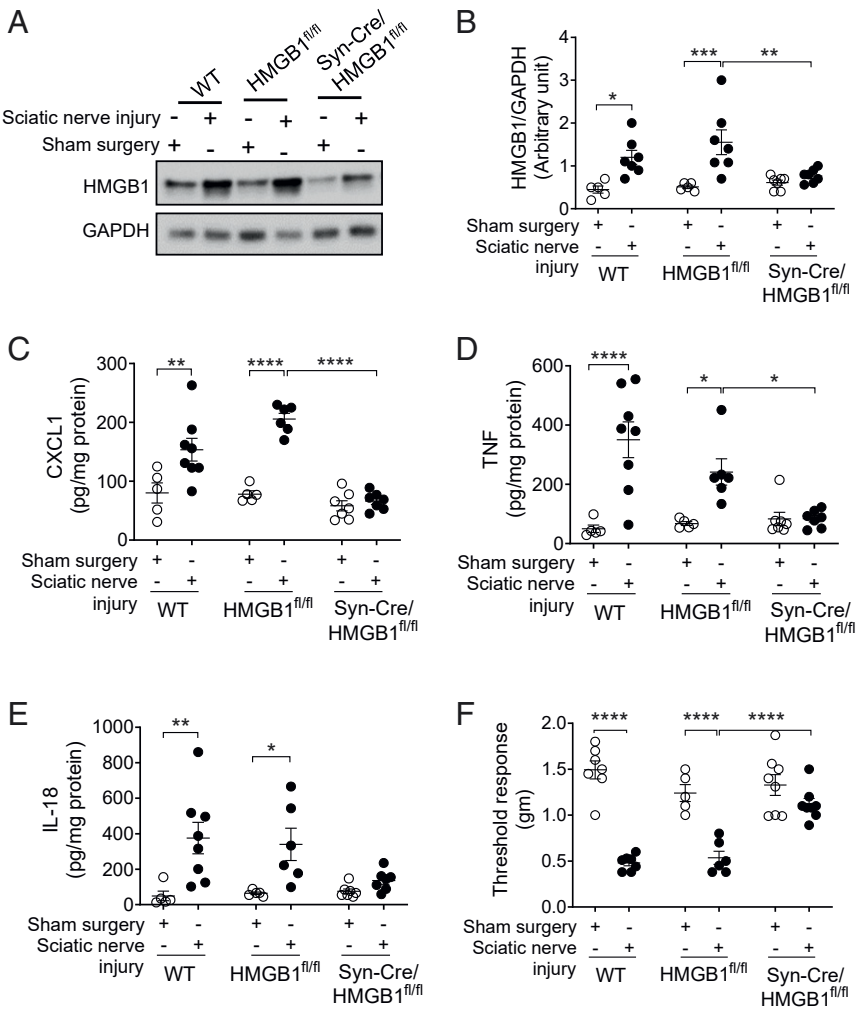

Fig. 2. Neuronal HMGB1 ablation leads to reduced local inflammation and hyperalgesia after sciatic nerve injury. (*A* and *B*) Sciatic nerve injury induces increase in HMGB1 levels. (*A*) WT ($n = 5$ to 7), HMGB1$^{fl/fl}$ ($n = 5$ to 6), or Syn-Cre/HMGB1$^{fl/fl}$ mice ($n = 7$) were subjected to sciatic nerve ligation surgery or sham surgery. Representative images of Western blot for HMGB1 and GAPDH in the paw tissues 2 wk postsurgery. (*B*) Ratio of HMGB1/GAPDH expression. Data are represented as individual mouse data points with mean ± SEM. Two-way ANOVA followed by Sidak's multiple comparisons test between groups: sham surgery vs. sciatic nerve injury (WT: $*P < 0.05$, HMGB1$^{fl/fl}$: $***P < 0.001$); sciatic nerve injury: HMGB1$^{fl/fl}$ vs. Syn-Cre/HMGB1$^{fl/fl}$ mice $**P < 0.01$. (*C–E*) Syn-Cre/HMGB1$^{fl/fl}$ mice mount reduced local chemokine and cytokines response. Levels of (*C*) CXCL1, (*D*) TNF, and (*E*) IL-18 in the paw tissues from WT ($n = 5$ to 8), HMGB1$^{fl/fl}$ ($n = 5$ to 6), or Syn-Cre/HMGB1$^{fl/fl}$ mice ($n = 7$). Data are represented as individual mouse data points with mean ± SEM. Two-way ANOVA followed by Sidak's multiple comparisons test between groups: $*P < 0.05$, $**P < 0.01$, $****P < 0.0001$. (*F*) Two weeks after sciatic nerve ligation surgery or sham surgery, mechanical hypersensitivity (von Frey) was assessed in WT ($n = 7$), HMGB1$^{fl/fl}$ ($n = 5$ to 6), or Syn-Cre/HMGB1$^{fl/fl}$ mice ($n = 8$). Data are represented as individual mouse data points with mean ± SEM. Two-way ANOVA followed by Sidak's multiple comparisons test between groups: $****P < 0.0001$.

are significantly reduced in Syn-Cre/HMGB1$^{fl/fl}$ mice as compared to HMGB1$^{fl/fl}$ mice (HMGB1$^{fl/fl}$ mice: CXCL1 = 317 ± 58, IL-6 = 146 ± 15, TNF = 162 ± 21, vs. Syn-Cre/HMGB1$^{fl/fl}$ mice; CXCL1 = 100 ± 16 [$P < 0.0001$], TNF = 38 ± 17 [$P < 0.01$] pg/mg protein) (Fig. 4 *F–H*, *SI Appendix*, Fig. S3 *F* and *G*). No significant differences are observed in IL-18 levels (IL-18 levels in HMGB1$^{fl/fl}$ = 66 ± 3 vs. Syn-Cre/HMGB1$^{fl/fl}$ = 66 ± 11 pg/mg protein) Fig. 4*I*, *SI Appendix*, Fig. S3*H*).

Significant reductions in immune cell infiltration, synovitis, pannus formation, and cartilage destruction are observed in Syn-Cre/HMGB1$^{fl/fl}$ mice as compared to WT and HMGB1$^{fl/fl}$ mice (histological score = 3.8 ± 0.1 in WT, 2.8 ± 0.4 in HMGB1$^{fl/fl}$ and 0.6 ± 0.2 in Syn-Cre/HMGB1$^{fl/fl}$, $P = 0.002$ vs. HMGB1$^{fl/fl}$ group) (Fig. 4 *J–K*). Because gender differences regarding neuropathic pain in rodents have been reported (61, 62), we also examined responses to CAIA in female WT, HMGB1$^{fl/fl}$, and Syn-Cre/HMGB1$^{fl/fl}$ mice (*SI Appendix*, Fig. S3 *A–H*). Selective ablation of neuronal HMGB1 in female mice also significantly delays the onset of arthritis and attenuates the severity of inflammation, hyperalgesia, and expression of inflammatory cytokines and chemokines (*SI Appendix*, Fig. S3 *A–H*). Together these results reveal a sex-independent role for neuronal HMGB1 in mediating inflammation, tissue damage, and hyperalgesia in experimental arthritis.

The results of these experiments establish that nociceptor-derived HMGB1 is a required mediator of inflammation and arthritis. Although numerous studies have previously implicated HMGB1 in inflammatory responses and in initiating neuropathic hyperalgesia following nerve injury, the cellular source of HMGB1 that contributes to a persistent inflammatory phenotype and to chronic hypersensitivity was previously unknown. Because global HMGB1 gene deletion is lethal to mice, and administration of HMGB1 antagonists cannot reveal the cellular source of HMGB1 release, here we developed neuronal-specific ablation to study the

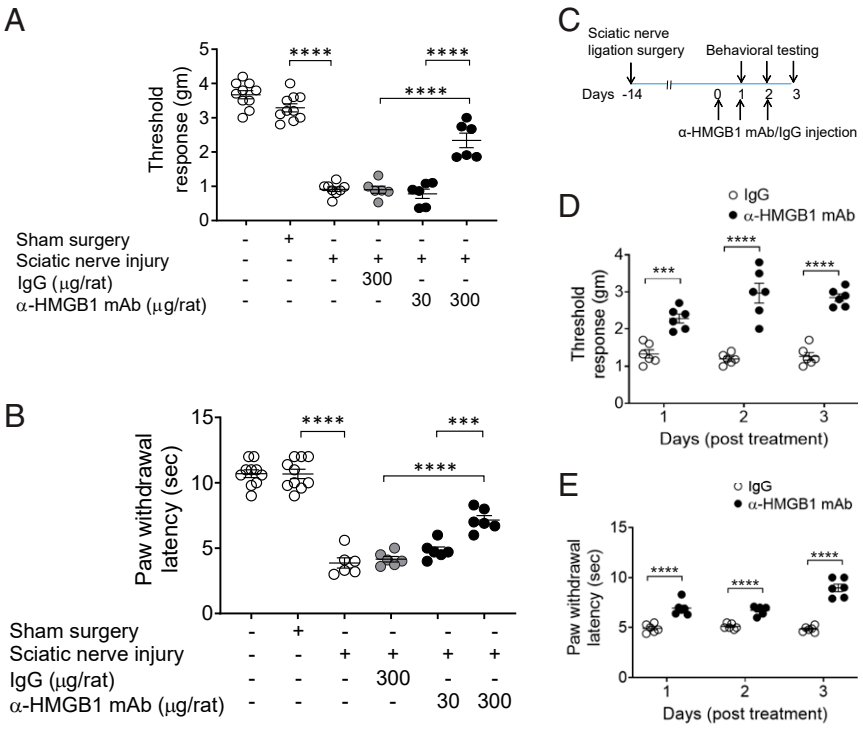

Fig. 3. Anti-HMGB1 mAb administration ameliorates sciatic nerve injury–induced hyperalgesia. (*A* and *B*) Female Wistar rats were subjected to sciatic nerve ligation surgery or sham surgery 2 wk prior to i.p. administration of anti-HMGB1 mAb (30 or 300 μg per rat) or control IgG (300 μg per rat). (*A*) Mechanical (von Frey) and (*B*) thermal (Hargreaves) hypersensitivity were assessed at 6 h after antibody was administered. Dose-dependent improvement in mechanical and thermal hypersensitivity is observed after anti-HMGB1 mAb administration. Data are represented as individual mouse data points with mean ± SEM. One-way ANOVA followed by Tukey's multiple comparisons test between groups: ***$P < 0.001$, ****$P < 0.0001$. $n = 10$ per group (normal or sham) and $n = 6$ (sciatic nerve injury). (*C–E*) Repetitive administration of anti-HMGB1 mAb ameliorates sciatic nerve injury–induced hyperalgesia. (*C*) Two weeks postsciatic nerve ligation or sham surgery, female Wistar rats received anti-HMGB1 mAb or IgG (300 μg/rat) i.p. once a day for 3 consecutive days. (*D*) Mechanical and (*E*) thermal hypersensitivity were assessed daily for 3 d after anti-HMGB1 mAb administration. Data are represented as individual mouse data points with mean ± SEM. Two-way ANOVA followed by Sidak's multiple comparisons test between groups: ***$P < 0.001$, ****$P < 0.0001$, $n = 6$ per group.

role of neuronal HMGB1 in arthritis and neuropathy. The selective ablation of neuronal HMGB1 in Syn-Cre/HMGB1$^{fl/fl}$ mice significantly attenuates inflammation and hyperalgesia and provides direct evidence for a critical role of neurons stimulating inflammation through release of HMGB1.

Following nerve injury, HMGB1 translocates from the nucleus into axons (63). The Syn-Cre/HMGB1$^{fl/fl}$ mice utilized here have pan-neuronal loss of HMGB1, which therefore includes higher-order neurons of the sensory system. The tactile allodynia which occurs following nociceptor injury is critically dependent on central neurons and their effects upon the microglial population within the spinal cord (64). In addition to a reduction in local inflammation, the beneficial effect of HMGB1 neutralization on pain behavior may extend to these higher-order neurons. In support of this concept, previous study of rats undergoing partial sciatic nerve ligation with subsequent mechanical allodynia has shown that neurons within the dorsal horn of the spinal cord (the second order neurons of the nociceptor system) increase synthesis of HMGB1. This augmented expression was associated with translocation of HMGB1 from the nucleus to the cytoplasm by neurons, but not in the surrounding astrocytes and microglia (65). Further, administration of HMGB1 antibody in this study significantly decreased the expression of the immediate early gene c-Fos within the dorsal horn, as well as of ionized calcium adapter protein 1, a specific marker of activated microglia, the cell type which mediates the development and maintenance of allodynia (64). Further study of how specific cell types involved in the neuroinflammation response in the acute and chronic stages of peripheral nerve injury is warranted.

It is important to note that neuronal release of HMGB1 may well confer advantageous or protective responses during the host response to infection or injury, when activation of inflammatory responses enhances host defense and promotes tissue repair. In the developing nervous system and after axonal damage, HMGB1 on the neuronal cell surface promotes axonal sprouting, neurite outgrowth, and neuronal migration. The findings of the present study now warrant assessing the functional role of sensory neuron-derived HMGB1 in the pathogenesis of other HMGB1-dependent infectious and sterile inflammatory disease models, including sepsis (35), pneumonia (66), epilepsy (67), neuropathic pain (68), cancer (69), and arthritis (70). It is also interesting to consider whether clinical observations of disease attenuation in rheumatoid arthritis and psoriatic arthritis patients following central or peripheral neurologic damage can be attributed to reduced release of neuronal HMGB1 (71–73).

In summary, our optogenetic and neuronal-specific ablation strategies applied to nerve-injury and arthritis models reveal a critical role for nociceptor HMGB1 in neuroinflammation and pain. Because neuron-derived HMGB1 is key to inflammatory responses and injury, this work suggests a paradigm for nervous system integration of environmental signals to stimulate inflammation as a fundamental mechanism of host defense during infection and injury. The results also suggest that targeting HMGB1 may constitute a new therapeutic approach for the treatment of a wide variety of diseases characterized by pain and inflammation.

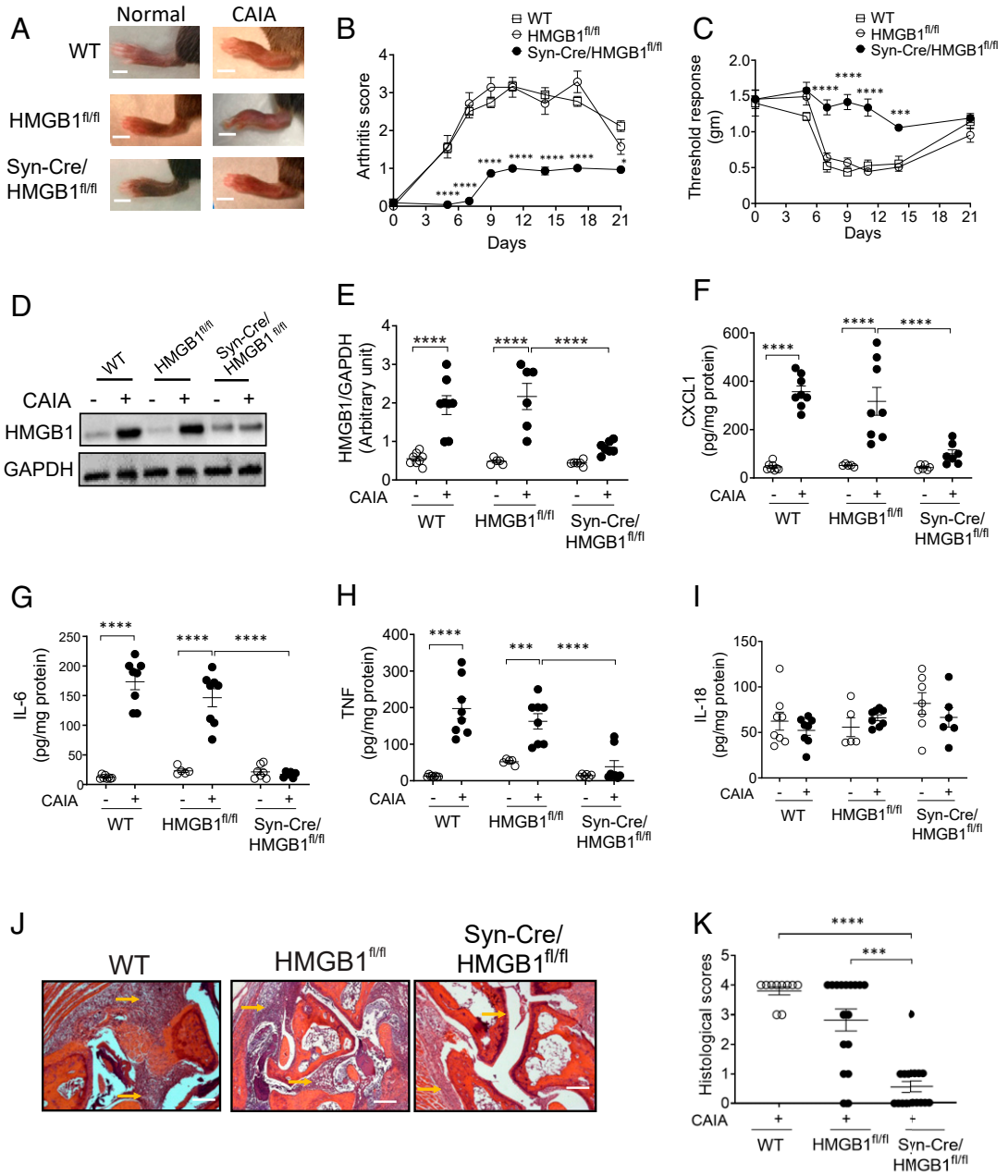

Fig. 4. Ablation of neuronal HMGB1 reduces joint inflammation and cartilage destruction and improves hyperalgesia in murine collagen antibody–induced arthritis. (*A* and *B*) Syn-Cre/HMGB1$^{fl/fl}$ mice are protected from CAIA. (*A*) Representative images of hind paws of WT, HMGB1$^{fl/fl}$, and Syn-Cre/HMGB1$^{fl/fl}$ mice on day 10 after initiation of arthritis. (Scale bar, 0.2 cm.) (*B*) Arthritis scores are significantly reduced in Syn-Cre/HMGB1$^{fl/fl}$ mice as compared to WT and HMGB1$^{fl/fl}$ mice. Data are represented as mean ± SEM. Two-way ANOVA followed by Sidak's multiple comparisons test between groups: Syn-Cre/HMGB1$^{fl/fl}$ vs. HMGB1$^{fl/fl}$ group: $*P < 0.05$, $****P < 0.0001$. (*C*) Mechanical hypersensitivity (von Frey) is significantly improved in Syn-Cre/HMGB1$^{fl/fl}$ mice subjected to CAIA as compared to WT and HMGB1$^{fl/fl}$ mice. Data are represented as mean ± SEM. Two-way ANOVA followed by Sidak's multiple comparisons test between groups: Syn-Cre/HMGB1$^{fl/fl}$ vs. HMGB1$^{fl/fl}$ group: $***P < 0.001$, $****P < 0.0001$. (*D* and *E*) HMGB1 levels are increased in the paw tissue in WT and HMGB1$^{fl/fl}$ mice but not in Syn-Cre/HMGB1$^{fl/fl}$ after CAIA. HMGB1 levels were assessed 10 d after initiation of arthritis in the paw tissues. (*D*) Representative images of Western blot for HMGB1 and GAPDH in the paw tissues post CAIA. (*E*) Ratio of HMGB1/GAPDH expression. Data are represented as individual mouse data points with mean ± SEM $n = 8$ (WT group), $n = 5$ to 6 (HMGB1$^{fl/fl}$), and $n = 6$ to 7 (Syn-Cre/HMGB1$^{fl/fl}$). Two-way ANOVA followed by Sidak's multiple comparisons test between groups: $****P < 0.0001$. (*F–I*) Syn-Cre/HMGB1$^{fl/fl}$ mice mount reduced local chemokine and cytokines response. Levels of (*F*) CXCL1, (*G*) IL-6, (*H*) TNF, and (*I*) IL-18 in the paw tissue from WT ($n = 8$), HMGB1$^{fl/fl}$ ($n = 5$ to 8) or Syn-Cre/HMGB1$^{fl/fl}$ mice ($n = 6$ to 7). Data are represented as individual mouse data points with mean ± SEM. Two-way ANOVA followed by Sidak's multiple comparisons test between groups: $***P < 0.001$, $****P < 0.0001$. (*J* and *K*) Histological assessment of joints on day 10 after initiation of arthritis. (*J*) Reduced infiltration of inflammatory cells, pannus formation, and cartilage damage (arrows) is observed in Syn-Cre/HMGB1$^{fl/fl}$ mice as compared to WT and HMGB1$^{fl/fl}$ subjected to CAIA. (Scale bars, 50 μm.) (*K*) The degree of inflammatory cells infiltration and cartilage disruption was graded as described in *Materials and Methods*. A significant reduction in histological score is observed in Syn-Cre/HMGB1$^{fl/fl}$ mice. $n = 10$ (WT), $n = 18$ (HMGB1$^{fl/fl}$ and Syn-Cre/HMGB1$^{fl/fl}$). Data are represented as individual mouse data points with mean ± SEM. One-way ANOVA followed by Tukey's multiple comparisons test between groups: $***P < 0.001$, $****P < 0.0001$.

Materials and Methods

Animals. All procedures with experimental animals were approved by the Institutional Animal Care and Use Committee and the Institutional Biosafety Committee of the Feinstein Institutes for Medical Research in accordance with NIH guidelines and the ethical guidelines of the International Association for the Study of Pain. Animals were maintained at 25 °C on a 12-h light/dark cycle with free access to food and water. Sprague-Dawley or Wistar rats, C57BL/6 mice, VGlut2-ires-Cre (*Slc17a6*$^{tm2(cre)Lowl}$/J), ChR2-YFP-flox mice (B6.Cg-*Gt(ROSA)26Sor*$^{tm32(CAG-COP4*H134R/EYFP)Hze}$/J), and synapsin^{Cre} mice (Syn-Cre, B6.Cg-Tg 671Jxm/J) were obtained from The Jackson Laboratory or Charles River Laboratories. HMGB1$^{fl/fl}$ mice were a gift from Timothy Billiar, University of Pittsburgh Medical Center, Pittsburgh, PA. Animals were acclimated for 7 d before any experimental use and housed under standard temperature, light/dark cycles. Mice (8 to 12 wk old) and rats (2 to 3 mo old) were used in these studies. VGlut2-ires-Cre mice were bred with ChR2-YFP-flox mice to generate Vglut2-Cre/ChR2-YFP mice that express ChR2 alleles under control of the *Vglut2* locus, which encodes vesicular glutamate transporter type 2 that is predominantly expressed in peripheral sensory neurons. Syn-Cre female mice were bred with HMGB1$^{fl/fl}$ male mice to generate Syn-Cre/HMGB1$^{fl/fl}$ mice. The genotypes of the transgenic strains were confirmed using PCR (Transnetyx).

Neuronal Cultures. DRG from adult Vglut2-Cre/ChR2-YFP mice and Syn-Cre/HMGB1$^{fl/fl}$ mice (8 to 12 wk) were dissected into neurobasal-A medium (Thermo Fisher Scientific) and dissociated in collagenase/dispase II (1 mg/mL, Sigma-Aldrich) at 37 °C for 90 min. After trituration to dissociate intact DRGs, cells were filtered with a 70-μm nylon cell strainer and centrifuged. After centrifugation, cells were suspended in neurobasal-A medium supplemented with neural growth factor (50 ng/mL, Sigma-Aldrich), B27 supplement (Thermo Fisher Scientific), penicillin (Thermo Fisher Scientific), and streptomycin (Thermo Fisher Scientific), plated on coverslips precoated with poly-L lysine (100 μg/mL, Sigma-Aldrich) and laminin (50 μg/mL, Sigma-Aldrich), and allowed to adhere for 12 to 15 h at 37 °C (with 5% CO_2).

Optogenetic Stimulation of DRGs. DRGs (L_1–L_6) were isolated from Vglut2-ChR2-YFP mice and cultured in poly-L lysine (100 μg/mL) and laminin (50 μg/mL) precoated chamber plates for 48 h. Cells were stimulated using 470 nm LED light (or control yellow light at 595 nm) at 20 Hz, and 10% duty cycle for 30 min using fiber-coupled LEDs (Thorlabs Inc). The supernatant was collected over time (for HMGB1 release) or for an additional 60-min incubation for measurements of LDH release (Sigma-Aldrich). For HMGB1 staining, cultured DRG cells were fixed with 4% paraformaldehyde (Thermo Fisher Scientific) followed by immunofluorescent staining with anti-HMGB1 antibody Alexa-555 (red, Abcam) and DAPI (blue) with endogenous VGlut2-YFP. Images were acquired using an LSM880 laser scanning confocal microscope (Zeiss). Levels of secreted HMGB1 in the supernatant were quantitated using an ELISA kit (IBL International).

Surgical Procedure. Ligation of the sciatic nerve was performed as described previously (49). Rats or mice were anesthetized by isoflurane inhalation (induction at 3 to 4% and maintenance at 1.5 to 2%), and the skin was shaved. Under aseptic conditions, a 1.5-cm incision was made on the skin at the midthigh level, followed by a small incision made dorsal to the pelvis. The biceps femoris and gluteous superficialis were separated, and the common sciatic nerve was exposed. Proximal to the sciatic trifurcation, about 5 to 7 mm of sciatic nerve was gently isolated and loosely ligated with four (for rats) or three (for mice) sutures (5/0 Ethicon chromic catgut suture). In sham control mice, the sciatic nerve was exposed but not ligated. Muscles were closed in layers and sutured with 4-0 silk, while the skin incision was closed using skin clips. Following surgery, animals were allowed to recover for 2 wk prior to any assessment.

CAIA in Mice. Arthritis was initiated in male and female mice (C57BL/6, HMGB1$^{fl/fl}$ or Syn-Cre/HMGB1$^{fl/fl}$, 7 to 9 wk of age) by injecting a mixture of five monoclonal antibodies against mouse type II collagen (Arthrogen-CIA Kit, Chondrex Inc.) (74) i.p. on day 0, followed by i.p. injection of lipopolysaccharide (LPS) at day 3 as per manufacturer's instructions. The development of joint inflammation in the fore and hind paws was monitored by visual inspection from days 0 to 21. The severity of arthritis was scored on a 0 to 4 scale: 0 = normal; 1 = mild, but definite redness and swelling of the ankle or wrist, or apparent redness and swelling limited to individual digits, regardless of the number of affected digits; 2 = moderate redness and swelling of ankle or wrist; 3 = severe redness and swelling of the entire paw including digits; and 4 = maximally inflamed limb involving multiple joints (74). In some experiments, animals were killed on day 10, the skin on the hindpaw and ankle joints was carefully removed, and joint, paws, and ankle joints along with surrounding tissues were collected and snap frozen at −20 °C for further analysis.

Behavioral Analysis. Animals were acclimatized to the behavioral testing apparatus used on at least three habituation sessions. At least three baseline measures were obtained for each behavioral test before testing. Mechanical sensitivity was measured using von Frey filaments and the Dixon up–down method to calculate the threshold response (75). Each animal was placed in a transparent box with a metal mesh floor and allowed to acclimate for 30 min before testing. The cage was elevated so that stimulation was applied to each hind paw from beneath the rodent. Calibrated von Frey filaments (capable of exerting forces of 0.4 to 7.3 g, Ugo Basile) were applied in ascending order on the plantar surface of the hind paw to define the threshold stimulus intensity required to elicit a paw withdrawal response. The duration of each stimulus was ∼5 to 7 s. The repetitive testing was performed with an interval of at least 5 min for the same paw. The behavioral responses were then used to calculate absolute threshold (50% probability of response), as described previously (76).

The paw withdrawal test was used to test the thermal hypersensitivity of rodents using a plantar analgesia instrument. Animals were placed in a transparent box and allowed to acclimate for 30 min before testing. A radiant heat source (Ugo Basile plantar test) was focused on the plantar surface of the hind paw; the time from switching on the radiant heat to paw withdrawal was measured automatically (53). The infrared heat intensity was adjusted as 50, and the cutoff latency at 15 s was used to prevent tissue damage. Each hind paw was tested three to four times with alternating paws, and with an interval of at least 5 min between tests. For some experiments, upon completion of behavioral testing, animals were killed, and tissue was collected for further analysis.

Histologic Analysis of CAIA Joints. Hind leg ankle joints from normal or CAIA mice (day 10 after CAIA initiation) were dissected and fixed in 4% paraformaldehyde. The joints were then decalcified (Newcomer Supply), embedded in paraffin, sectioned at 5 μm, and stained with hematoxylin and eosin. The degree of inflammatory cell infiltration and cartilage disruption was graded on a 0 to 4 scale as described previously (77) with some modification: 0 = normal; 1 = mild inflammatory cell infiltration/cartilage degradation; 2 = mild to moderate inflammatory cells infiltration/cartilage degradation; 3 = severe inflammatory cell infiltration/cartilage degradation; and 4 = maximal inflammatory cell infiltration/cartilage degradation. All tissues were scored in a blinded manner.

Immunohistochemistry. Mice were anesthetized and intracardially perfused with cold phosphate-buffered saline (PBS) followed by 4% paraformaldehyde. Lumbar and thoracic DRGs, brain, and spleen were harvested, fixed in 4% paraformaldehyde overnight at 4 °C, and then cryoprotected in 30% sucrose for 48 h. Tissues were embedded in optimal cutting temperature compound (VWR International), and 14-μm sections were collected on slides and stored at −20 °C until further analyses. For HMGB1 staining, frozen sections were air dried for 30 min and fixed with 4% paraformaldehyde for 15 min. After a PBS wash, the sections were blocked with antibody host serum (10% rabbit or mouse serum, 0.3% TX-100 in PBS) for 1 h at room temperature, followed by staining with primary antibodies at 4 °C overnight, rinsed three times with PBS, and mounted using Vectashield anti-fade mounting medium with DAPI (Vector Laboratories). The antibodies used were Alexa Fluor 555–conjugated anti-HMGB1 rabbit antibody at 1:200 dilution (Abcam), Alexa Fluor 647–conjugated anti-CD3 rat monoclonal antibody at 1:100 dilution (BioLegend), and Alexa Fluor 594– or 647–conjugated anti-NeuN antibody at 1:100 dilution (Abcam). Fluorescence images were acquired on a confocal microscope (Zeiss LSM880) and analyzed using FIJI software.

Measurements of HMGB1, Chemokines, and Cytokines. Frozen tissues (paws and joints obtained from the normal or injured side) were homogenized in PBS with protease inhibitor (Sigma-Aldrich). Protein concentration was measured using the Bradford assay (BioRad, Inc.). Levels of TNF, CXCL1, IL-18, and IL-6 were measured using commercial ELISA kits per manufacturer's instructions (R&D System). HMGB1 was measured by Western blotting (40 μg protein per lane) with anti-HMGB1 monoclonal antibodies (2G7 at 1 μg/mL final concentration). Membranes were also stained using anti-GAPDH antibodies (Abcam) as a loading control. In some experiments, HMGB1 levels were measured using ELISA (IBL International).

Preparations of Anti-HMGB1 Monoclonal Antibodies. Anti-HMGB1 monoclonal antibodies (mAb 2G7) were generated as described previously (52). As

controls, mouse IgG was used. The LPS content in protein solutions was less than 10 pg/mg protein as measured by the Limulus assay.

Statistical Analysis. Data were analyzed using GraphPad Prism software. Differences between groups were analyzed using one-way ANOVA followed with Tukey's or Sidak's multiple comparison test, or two-way ANOVA followed by Sidak's multiple comparison tests. For all analyses, $P \leq 0.05$ was considered statistically significant.

Data Availability. All study data are included in the article and/or *SI Appendix*.

ACKNOWLEDGMENTS. This study was supported by grants from the NIH: National Institute of General Medical Services (NIGMS) R35GM118182 (K.J.T.), NIGMS R01GM132672 (S.S.C.), NIGMS 1R01GM128008-01 (V.A.P.), NIGMS R01GM063075 (H.W.); National Institute of Allergy and Infectious Diseases P01AI102852 (S.S.C. and K.J.T.); and National Center of Complementary and Integrative Health R01AT005076 (H.W.).

1. J. M. Pearce, Sir Charles Scott Sherrington (1857-1952) and the synapse. *J. Neurol. Neurosurg. Psychiatry* **75**, 544 (2004).
2. R. E. Burke, Sir Charles Sherrington's the integrative action of the nervous system: a centenary appreciation. *Brain* **130**, 887–894 (2007).
3. F. A. Pinho-Ribeiro, W. A. Verri, Jr, I. M. Chiu, Nociceptor sensory neuron-immune interactions in pain and inflammation. *Trends Immunol.* **38**, 5–19 (2017).
4. S. S. Chavan, P. Ma, I. M. Chiu, Neuro-immune interactions in inflammation and host defense: Implications for transplantation. *Am. J. Transplant.* **18**, 556–563 (2018).
5. H. A. Silverman, A. Chen, N. L. Kravatz, S. S. Chavan, E. H. Chang, Involvement of neural transient receptor potential channels in peripheral inflammation. *Front. Immunol.* **11**, 2742 (2020).
6. I. M. Chiu, C. A. von Hehn, C. J. Woolf, Neurogenic inflammation and the peripheral nervous system in host defense and immunopathology. *Nat. Neurosci.* **15**, 1063–1067 (2012).
7. I. M. Chiu *et al*., Bacteria activate sensory neurons that modulate pain and inflammation. *Nature* **501**, 52–57 (2013).
8. S. Talbot *et al*., Silencing nociceptor neurons reduces allergic airway inflammation. *Neuron* **87**, 341–354 (2015).
9. P. Baral *et al*., Nociceptor sensory neurons suppress neutrophil and γδ T cell responses in bacterial lung infections and lethal pneumonia. *Nat. Med.* **24**, 417–426 (2018).
10. C. L. Barberini, S. E. Morrison, A. Saez, B. Lau, C. D. Salzman, Complexity and competition in appetitive and aversive neural circuits. *Front. Neurosci.* **6**, 170 (2012).
11. Y.-Q. Cai, W. Wang, A. Paulucci-Holthauzen, Z. Z. Pan, Brain circuits mediating opposing effects on emotion and pain. *J. Neurosci.* **38**, 6340–6349 (2018).
12. J. D. Wood, The first nobel prize for integrated systems physiology: Ivan Petrovich Pavlov, 1904. *Physiology (Bethesda)* **19**, 326–330 (2004).
13. C. A. Janeway Jr, Approaching the asymptote? Evolution and revolution in immunology. *Cold Spring Harb. Symp. Quant. Biol.* **54**, 1–13 (1989).
14. S. B. McMahon, F. La Russa, D. L. H. Bennett, Crosstalk between the nociceptive and immune systems in host defence and disease. *Nat. Rev. Neurosci.* **16**, 389–402 (2015).
15. S. S. Chavan, K. J. Tracey, Essential neuroscience in immunology. *J. Immunol.* **198**, 3389–3397 (2017).
16. S. S. Chavan, V. A. Pavlov, K. J. Tracey, Mechanisms and therapeutic relevance of neuro-immune communication. *Immunity* **46**, 927–942 (2017).
17. K. J. Tracey, The inflammatory reflex. *Nature* **420**, 853–859 (2002).
18. V. A. Pavlov, S. S. Chavan, K. J. Tracey, Molecular and functional neuroscience in immunity. *Annu. Rev. Immunol.* **36**, 783–812 (2018).
19. M. Rosas-Ballina *et al*., Splenic nerve is required for cholinergic antiinflammatory pathway control of TNF in endotoxemia. *Proc. Natl. Acad. Sci. U.S.A.* **105**, 11008–11013 (2008).
20. A. M. Kressel *et al*., Identification of a brainstem locus that inhibits tumor necrosis factor. *Proc. Natl. Acad. Sci. U.S.A.* **117**, 29803–29810 (2020).
21. M. Rosas-Ballina *et al*., Acetylcholine-synthesizing T cells relay neural signals in a vagus nerve circuit. *Science* **334**, 98–101 (2011).
22. H. Wang *et al*., Nicotinic acetylcholine receptor alpha7 subunit is an essential regulator of inflammation. *Nature* **421**, 384–388 (2003).
23. P. S. Olofsson *et al*., α7 nicotinic acetylcholine receptor (α7nAChR) expression in bone marrow-derived non-T cells is required for the inflammatory reflex. *Mol. Med.* **18**, 539–543 (2012).
24. F. A. Koopman, *et al*., Vagus nerve stimulation inhibits cytokine production and attenuates disease severity in rheumatoid arthritis. **113**, 8284–8289 (2016).
25. B. Bonaz *et al*., Chronic vagus nerve stimulation in Crohn's disease: A 6-month follow-up pilot study. *Neurogastroenterol. Motil.* **28**, 948–953 (2016).
26. M. C. Genovese, *et al*., Safety and efficacy of neurostimulation with a miniaturised vagus nerve stimulation device in patients with multidrug-refractory rheumatoid arthritis: A two-stage multicentre, randomised pilot study. *Lancet Rheumatol.* **2**, e527–e538 (2020).
27. U. Andersson, K. J. Tracey, HMGB1 is a therapeutic target for sterile inflammation and infection. *Annu. Rev. Immunol.* **29**, 139–162 (2011).
28. H. Yang, H. Wang, S. S. Chavan, U. Andersson, High mobility group box protein 1 (HMGB1): The prototypical endogenous danger molecule. *Mol. Med.* **21** (suppl. 1), S6–S12 (2015).
29. N. Kayagaki *et al*., Non-canonical inflammasome activation targets caspase-11. *Nature* **479**, 117–121 (2011).
30. H. Yang *et al*., A critical cysteine is required for HMGB1 binding to Toll-like receptor 4 and activation of macrophage cytokine release. *Proc. Natl. Acad. Sci. U.S.A.* **107**, 11942–11947 (2010).
31. U. Andersson, H. Yang, H. Harris, Extracellular HMGB1 as a therapeutic target in inflammatory diseases. *Expert Opin. Ther. Targets* **22**, 263–277 (2018).
32. H. Yang, H. Wang, U. Andersson, Targeting inflammation driven by HMGB1. *Front. Immunol.* **11**, 484 (2020).
33. D. Messmer *et al*., High mobility group box protein 1: an endogenous signal for dendritic cell maturation and Th1 polarization. *J. Immunol.* **173**, 307–313 (2004).
34. R. Saenz *et al*., TLR4-dependent activation of dendritic cells by an HMGB1-derived peptide adjuvant. *J. Transl. Med.* **12**, 1–11 (2014).
35. H. Wang *et al*., HMG-1 as a late mediator of endotoxin lethality in mice. *Science* **285**, 248–251 (1999).
36. T. Östberg *et al*., Protective targeting of high mobility group box chromosomal protein 1 in a spontaneous arthritis model. *Arthritis Rheum.* **62**, 2963–2972 (2010).
37. M. D. Laird *et al*., High mobility group box protein-1 promotes cerebral edema after traumatic brain injury via activation of toll-like receptor 4. *Glia* **62**, 26–38 (2014).
38. G. Faraco *et al*., High mobility group box 1 protein is released by neural cells upon different stresses and worsens ischemic neurodegeneration in vitro and in vivo. *J. Neurochem.* **103**, 590–603 (2007).
39. M. Shibasaki *et al*., Induction of high mobility group box-1 in dorsal root ganglion contributes to pain hypersensitivity after peripheral nerve injury. *Pain* **149**, 514–521 (2010).
40. P. Feldman, M. R. Due, M. S. Ripsch, R. Khanna, F. A. White, The persistent release of HMGB1 contributes to tactile hyperalgesia in a rodent model of neuropathic pain. *J. Neuroinflammation* **9**, 180 (2012).
41. Q. Wang *et al*., Ethyl pyruvate attenuates spinal cord ischemic injury with a wide therapeutic window through inhibiting high-mobility group box 1 release in rabbits. *Anesthesiology* **110**, 1279–1286 (2009).
42. X. Wang *et al*., Ethanol directly induced HMGB1 release through NOX2/NLRP1 inflammasome in neuronal cells. *Toxicology* **334**, 104–110 (2015).
43. T. Maeda, M. Ozaki, Y. Kobayashi, N. Kiguchi, S. Kishioka, HMGB1 as a potential therapeutic target for neuropathic pain. *J. Pharmacol. Sci.* **123**, 301–305 (2013).
44. N. M. Agalave, C. I. Svensson, Extracellular high-mobility group box 1 protein (HMGB1) as a mediator of persistent pain. *Mol. Med.* **20**, 569–578 (2015).
45. E. S. Boyden, F. Zhang, E. Bamberg, G. Nagel, K. Deisseroth, Millisecond-timescale, genetically targeted optical control of neural activity. *Nat. Neurosci.* **8**, 1263–1268 (2005).
46. P. Brumovsky, M. Watanabe, T. Hökfelt, Expression of the vesicular glutamate transporters-1 and -2 in adult mouse dorsal root ganglia and spinal cord and their regulation by nerve injury. *Neuroscience* **147**, 469–490 (2007).
47. P. Kumar, A. Nagarajan, P. D. Uchil, Analysis of cell viability by the lactate dehydrogenase assay. *Cold Spring Harb. Protoc.* **2018**, 465–468 (2018).
48. S. Calogero *et al*., The lack of chromosomal protein Hmg1 does not disrupt cell growth but causes lethal hypoglycaemia in newborn mice. *Nat. Genet.* **22**, 276–280 (1999).
49. G. J. Bennett, Y. K. Xie, A peripheral mononeuropathy in rat that produces disorders of pain sensation like those seen in man. *Pain* **33**, 87–107 (1988).
50. M. A. R. C. Daemen *et al*., Neurogenic inflammation in an animal model of neuropathic pain. *Neurol. Res.* **20**, 41–45 (1998).
51. Y. W. Lin, T. J. Tseng, W. M. Lin, S. T. Hsieh, Cutaneous nerve terminal degeneration in painful mononeuropathy. *Exp. Neurol.* **170**, 290–296 (2001).
52. S. Qin *et al*., Role of HMGB1 in apoptosis-mediated sepsis lethality. *J. Exp. Med.* **203**, 1637–1642 (2006).
53. K. Hargreaves, R. Dubner, F. Brown, C. Flores, J. Joris, A new and sensitive method for measuring thermal nociception in cutaneous hyperalgesia. *Pain* **32**, 77–88 (1988).
54. H. E. Harris, U. Andersson, D. S. Pisetsky, HMGB1: a multifunctional alarmin driving autoimmune and inflammatory disease. *Nat. Rev. Rheumatol.* **8**, 195–202 (2012).
55. J. Z. B. Cher *et al*., Alarmins in frozen shoulder: A molecular association between inflammation and pain. *Am. J. Sports Med.* **46**, 671–678 (2018).
56. F. G. Thankam, M. F. Dilisio, N. E. Dietz, D. K. Agrawal, TREM-1, HMGB1 and RAGE in the shoulder tendon: Dual mechanisms for inflammation based on the coincidence of glenohumeral arthritis. *PLoS One* **11**, e0165492 (2016).
57. R. Kokkola *et al*., High mobility group box chromosomal protein 1: a novel proinflammatory mediator in synovitis. *Arthritis Rheum.* **46**, 2598–2603 (2002).
58. K. S. Nandakumar, L. Svensson, R. Holmdahl, Collagen type II-specific monoclonal antibody-induced arthritis in mice: description of the disease and the influence of age, sex, and genes. *Am. J. Pathol.* **163**, 1827–1837 (2003).
59. A. Bersellini Farinotti *et al*., Cartilage-binding antibodies induce pain through immune complex-mediated activation of neurons. *J. Exp. Med.* **216**, 1904–1924 (2019).
60. É. Borbély *et al*., Complex role of capsaicin-sensitive afferents in the collagen antibody-induced autoimmune arthritis of the mouse. *Sci. Rep.* **8**, 15916 (2018).
61. A. Nazarian, J. M. Tenayuca, F. Almasarweh, A. Armendariz, D. Are, Sex differences in formalin-evoked primary afferent release of substance P. *Eur. J. Pain* **18**, 39–46 (2014).
62. J. C. S. Mapplebeck, S. Beggs, M. W. Salter, Sex differences in pain: A tale of two immune cells. *Pain*, **157**, S2–S6 (2016).
63. T. T. Merianda *et al*., Axonal amphoterin mRNA is regulated by translational control and enhances axon outgrowth. *J. Neurosci.* **35**, 5693–5706 (2015).
64. M. Tsuda *et al*., P2X4 receptors induced in spinal microglia gate tactile allodynia after nerve injury. *Nature* **424**, 778–783 (2003).

65. Y. Nakamura *et al*., Neuropathic pain in rats with a partial sciatic nerve ligation is alleviated by intravenous injection of monoclonal antibody to high mobility group box-1. *PLoS One* **8**, e73640 (2013).
66. N. Nosaka *et al*., Anti-high mobility group box-1 monoclonal antibody treatment provides protection against influenza A virus (H1N1)-induced pneumonia in mice. *Crit. Care* **19**, 1–9 (2015).
67. M. Maroso *et al*., Toll-like receptor 4 and high-mobility group box-1 are involved in ictogenesis and can be targeted to reduce seizures. *Nat. Med.* **16**, 413–419 (2010).
68. N. M. Agalave *et al*., Spinal HMGB1 induces TLR4-mediated long-lasting hypersensitivity and glial activation and regulates pain-like behavior in experimental arthritis. *Pain* **155**, 1802–1813 (2014).
69. W. Tong *et al*., Spinal high-mobility group box 1 contributes to mechanical allodynia in a rat model of bone cancer pain. *Biochem. Biophys. Res. Commun.* **395**, 572–576 (2010).
70. D. S. Pisetsky, H. Erlandsson-Harris, U. Andersson, High-mobility group box protein 1 (HMGB1): an alarmin mediating the pathogenesis of rheumatic disease. *Arthritis Res. Ther.* **10**, 1–10 (2008).
71. S. Hamilton, Unilateral rheumatoid arthritis in hemiplegia. *J. Can. Assoc. Radiol.* **34**, 49–50 (1983).
72. E. N. Glick, Asymmetrical rheumatoid arthritis after poliomyelitis. *BMJ* **3**, 26–28 (1967).
73. I. Yaghmai, S. M. Rooholamini, H. F. Faunce, Unilateral rheumatoid arthritis: protective effect of neurologic deficits. *AJR Am. J. Roentgenol.* **128**, 299–301 (1977).
74. P. Hutamekalin *et al*., Collagen antibody-induced arthritis in mice: development of a new arthritogenic 5-clone cocktail of monoclonal anti-type II collagen antibodies. *J. Immunol. Methods* **343**, 49–55 (2009).
75. S. R. Chaplan, F. W. Bach, J. W. Pogrel, J. M. Chung, T. L. Yaksh, Quantitative assessment of tactile allodynia in the rat paw. *J. Neurosci. Methods* **53**, 55–63 (1994).
76. E. D. Milligan *et al*., Thermal hyperalgesia and mechanical allodynia produced by intrathecal administration of the human immunodeficiency virus-1 (HIV-1) envelope glycoprotein, gp120. *Brain Res.* **861**, 105–116 (2000).
77. A. Mencarelli *et al*., Solomonsterol A, a marine pregnane-X-receptor agonist, attenuates inflammation and immune dysfunction in a mouse model of arthritis. *Mar. Drugs* **12**, 36–53 (2013).